SUPPRESSION OF VORTEX STRETCHING AND GENERATION OF ACOUSTIC/KELVIN WAVES IN COMPRESSIBLE HOMOGENEOUS TURBULENCE

Hideaki Miura
Theory and Computer Simulation Center,
National Institute for Fusion Science
322-6 Oroshi, Toki, Gifu 509-5292, Japan
miura@toki.theory.nifs.ac.jp

ABSTRACT

Vortex structures in compressible isotropic turbulence are compared to those in incompressible isotropic turbulence in order to elucidate compressibility effects on vortices. It is shown that vortex cross-sections, vortex circulations, and some other quantities which characterize strength of swirling motions of vortices are suppressed by compressibility. The suppressions are attributed to effects of the density variations in the initial stage of vortex formation and succeeding reduction of the vortex stretching. It is also shown that waves excited on vortices are considerably changed by existence of compressibility.

INTRODUCTION

Compressibility effects on turbulence have been investigated extensively. It is well known that compressibility suppresses growth of the turbulent kinetic energy in homogeneous turbulent shear flows or mixing layer width in planar mixing layers.(Lele, 1994) There are also some observations that detailed structures of turbulence can be modified by compressibility. For example, turbulence often generates shocklets, which are intrinsic to compressible fluids.(Lee et al. 1991)

Works in this one decade have revealed a great deal of nature of compressible turbulence. Sarkar(1995) has shown that changes of the incompressible components of the Reynolds shear anisotropy is more important than some compressible-fluid-intrinsic terms in the energy budget equation, such as the pressure-dilatation and dilatational dissipation, to explain the reduction of the growth rate of the kinetic energy in homogeneous shear turbulence. Vreman et. al(1996) have shown that suppression of pressure fluctuation is crucial to elucidate compressibility effects on evolutions f planar mixing layers. Though these two and succeeding works present clear explanations on compressibility effects on turbulence, detailed physical process which bring about these phenomena are not given in them, unfortunately.

The purpose of our research is to clarify how compressibility changes small-scale structures of turbulence. For this purpose, we restrict ourselves to isotropic turbulence which is highly idealized and easier to analyze than homogeneous shear turbulence or planar mixing layers. A special attention is paid to vortex structures because they are good representatives of incompressible motions of fluids. Modification of the vortex structures by compressibility should have significant effects on structures of turbulence. We conduct direct numerical simulations (DNS) of decaying isotropic turbulence of compressible and incompressible fluids and compare vortex structures in the two kinds of fluids. In §2, outlines of our DNS are described. In §3, results of vortex analysis are shown. Concluding remarks are shown in §4.

DIRECT NUMERICAL SIMULATION

We simulate motions of fluids by solving systems of governing equations of compressible and incompressible fluids in $(2\pi)^3$ triply-periodic box by the pseudo-spectral and Runge-Kutta-Gill scheme. Motions of compressible fluids are described by the equations of density ρ, momentum ρu_i and total energy E_T as follows.

$$\frac{\partial \rho}{\partial t} = -\frac{\partial (\rho u_i)}{\partial x_i} \tag{1}$$

$$\frac{\partial (\rho u_i)}{\partial t} = -\frac{\partial (\rho u_i u_j)}{\partial x_j} - \frac{\partial p}{\partial x_i} + \frac{2}{Re_0}\frac{\partial}{\partial x_j}\tau_{ij} \quad (i = 1,2,3) \tag{2}$$

$$\frac{\partial E_T}{\partial t} = -\frac{\partial}{\partial x_i}[(E_T + p)u_i] + \frac{1}{{M_0}^2 Pr_0 Re_0(\gamma - 1)}\frac{\partial^2 T}{\partial x_i \partial x_i} + \frac{2}{Re_0}\frac{\partial}{\partial x_j}(u_i \tau_{ij}) \tag{3}$$

$$\tau_{ij} = S_{ij} - \frac{1}{3}\delta_{ij}\left(\frac{\partial u_k}{\partial x_k}\right) \tag{4}$$

$$E_T = \frac{p}{\gamma - 1} + \frac{1}{2}\rho u_i u_i \tag{5}$$

Here u_i, S_{ij}, p and T are the i-th component of the velocity vector $\mathbf{u}$, (i,j) component of the rate of the strain tensor $\mathbf{S}$, pressure and temperature, respectively. We assume that the compressible fluid obeys the equation of an ideal gas $p = \rho T/\gamma M_0^2$, where the ratio of the specific heats is $\gamma = 1.4$. The equations (1)-(5) are already normalized so that the equations coincide with the incompressible Navier-Stokes equation (described below) in the incompressible limit. Refer to Kida and Orszag(1990) or Miura and Kida(1994) for details of normalization of equations and numerical scheme.

Motions of an incompressible fluid with a constant density is described by the equation of continuity and the incompressible Navier-Stokes equation as follows.

$$\frac{\partial u_i}{\partial x_i} = 0 \tag{6}$$

$$\frac{\partial u_i}{\partial t} = -u_j\frac{\partial u_i}{\partial x_j} - \frac{\partial p}{\partial x_i} + \frac{1}{Re_0}\frac{\partial^2 u_i}{\partial x_j \partial x_j} \quad (i = 1,2,3) \tag{7}$$

In the system of equations, we have only one control parameters: Reynolds number Re_0.

Outlines of our DNS are as follows. Control parameters, number of grid points N^3 and $k_{max}\eta$, an index of numerical

Table 1: Control parameters of DNS. Symbols k_{max} and η represents the maximum wavenumber available in the DNS and the Kolmogorov length scale, respectively.

	N^3	Re_0	M_0^2	Pr_0	γ	$k_{max}\eta$
C1	512^3	1000	2.0	0.70	1.4	2.0
C2	512^3	1000	0.5	0.70	1.4	2.0
C3	512^3	1000	0.1	0.70	1.4	2.0
C4	1024^3	2000	2.0	0.70	1.4	2.0
I1	256^3	1000	-	-	-	2.0
I2	512^3	2000	-	-	-	2.0

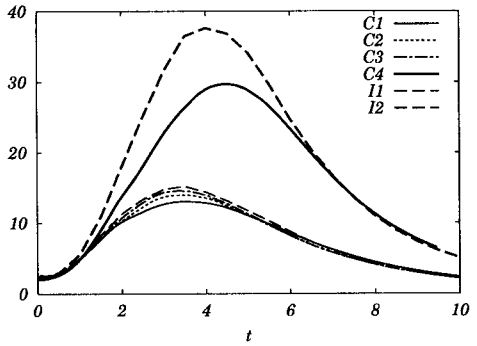

Figure 1: Time evolutions of the enstrophy density. Thick (thin) lines represent graphs of $Re_0 = 2000$ (1000) runs.

resolution, are shown in Table 1. In the column of $k_{max}\eta$, minimum values of each runs are shown. The Taylor's length scale Reynolds number of $Re_0 = 2000$ (1000) runs decay from 280(140) to 40(40). Since we set the initial density fluctuation and dilatation be null in the compressible runs, compressibility of these runs remain relatively weak. The turbulent Mach number is typically 0.4 for $M_0^2 = 2$ runs and we do not observe shocklet.

In our DNS, differences of the kinetic energies among compressible and incompressible runs are not very large. In Fig.1, time evolutions of the enstrophy are shown. The reduction of the enstrophy from run I2 to C4 (I1 to C1) is about 11% (2.5%). The reductions look relatively small, especially for low-Re_0 runs. However, the root-mean-square (rms) fluctuation of the enstrophy density from run I2 to C4 (I1 to C1) is 20% (15%) (the figure is not shown), which is larger than the reduction of the enstrophy. Especially, the reduction in low Re_0 runs are quite clear. Note that the pressure fluctuations are also reduced by compressibility. Since fluctuations of the enstrophy and pressure are strongly related with vortex structures, it suggests that the vortex structures should be sensitively changed by compressibility effect.

VORTEX ANALYSIS

Compressibility effects on vortices

In most cases below, we show only data of $Re_0 = 1000$ because we do not have runs with intermediate M_0 for $Re_0 = 2000$ simulations. However, as have been shown above, runs with the lower Re_0 show clear compressibility effects on vortices.

We identify tubular vortices by the use of the scheme developed by Miura and Kida(1997), and Kida and Miura (1998a). We extract central axes of vortices and regions where streamlines relative to each vortex axis are elliptical (vortex cores). We make use of two advantages of our scheme. One advantage is that we do not need any arbitrary parameter such as the thresholds of isosurfaces of the enstrophy density or $\nabla^2 p$, which are often used to visualize vortices. Therefore, we are able to identify vortices in an objective manner, whether the swirling motions of vortices are strong or weak. Another advantage is that we identify individual vortices separately. It enables us to compare detailed properties of compressible and incompressible vortices which shares their ancestor in the initial condition.

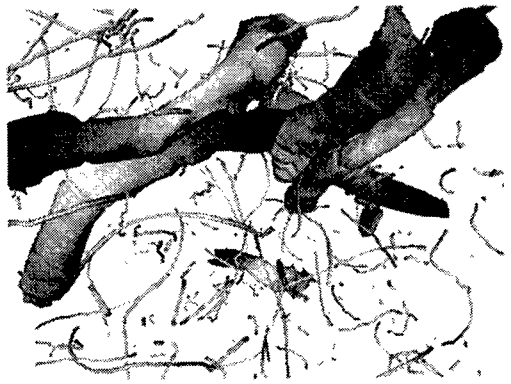

Figure 2: Vortex axes and a few typical vortex cores in run C1.

In Fig.2, vortex axes and a few typical vortex cores of run C1 are shown. A region of 128^3 grid points is shown. In the course of the time evolution, length of vortex axes grows almost monotonically in time. The volume occupied by vortex cores decays till $t = 2.5$ and begins to increase after that (Miura, 2002).

In Fig.3, the probability density functions (pdfs) of vortex core radii in runs C1-C3 and I1 at $t = 3.5$ are shown. Though it is difficult to distinguish plots of the pdfs of compressible runs (especially between C2 and C3), differences between pdfs of compressible runs and the pdf of run I1 are clear. Apparently, compressible runs have smaller core radii than the incompressible run. The the central value of the pdf of run I1 is about 5η, being consistent with earlier results (Jiménez et al. 1993, Kida and Miura 1998a). The central values of runs C1, C2 and C3 are about 4η. Compressibility reduces the extent of vortices about 20%.

Since the extent of vortices are closely related with

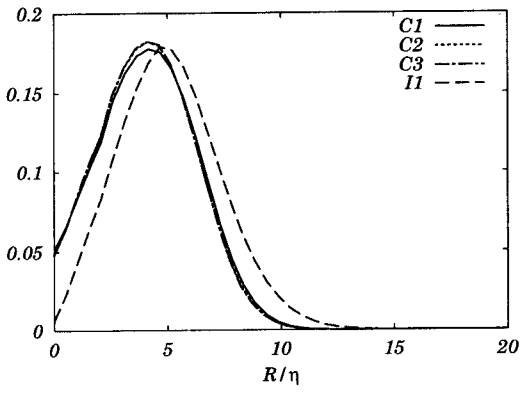

Figure 3: Pdfs of vortex core radii of runs C1-C3 and I1 at $t = 3.5$.

strength of swirling motions of vortices, we investigate how it is affected by compressibility. We characterize the strength of swirling motions by the longitudinal vorticity $\omega_{\|}$. Time evolutions of $\left\langle \omega_{\|}^2 \right\rangle_A$ is shown in Fig.4(a), where $\langle\cdot\rangle_A$ represents the average along all of the vortex axes. The quantity $\left\langle \omega_{\|}^2 \right\rangle_A$ is reduced about 30% from run I1 to C1. In Fig.4(b), time evolutions of the vortex circulation $\left\langle \omega_\Gamma^2 \right\rangle_A = \left\langle (\Gamma/S)^2 \right\rangle_A$ are shown where $\Gamma = \oint_C \mathbf{u} \cdot d\mathbf{l}$ and S are the circulation and cross-section of a vortex, respectively. The outer most boundaries of vortex cores are adopted as closed paths to calculate the line integral $\oint_C \cdot d\mathbf{l}$. Figs.4(b) also shows that strength of swirling motions are reduced by compressibility.

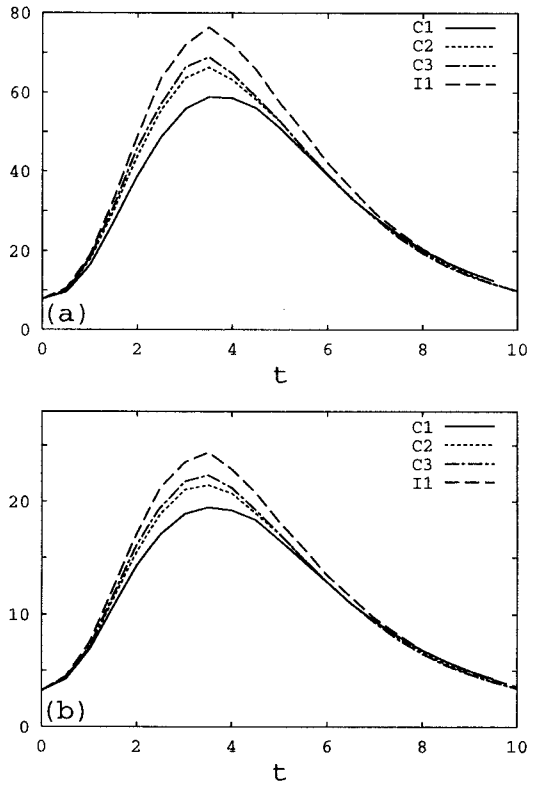

Figure 4: Time evolutions of the averages of (a)$\left\langle \omega_{\|}^2 \right\rangle_A$ and (b)$\left\langle \omega_\Gamma^2 \right\rangle_A$.

As has been described in the Introduction, we consider that changes of vortex structures should be considerably responsible to the suppressions of the kinetic growth and/or that of the pressure fluctuation. Vortices contribute to generate pressure fluctuation through decrease of pressure on the plane of their swirling motions. The pressure fluctuation caused by the swirling motions are well represented by the incompressible component of the pressure p^I, which is given by

$$\nabla^2 p^I = -\frac{\partial^2}{\partial x_i \partial x_j}\left(u_i^I u_j^I\right) \tag{8}$$

The superscript ^{I} represents the incompressible component of the quantity. Recall that the right-hand-side of eq.(8) is nothing but an operation to the incompressible components of the Reynolds shear stress which Sarkar(1995) has argued. Changes of Reynolds shear stress and pressure fluctuation are coupled by the vortex structures as shown in eq.(8).

In Fig.5, the averaged values of (a)$\omega_{\|}$ and (b)p^I are shown as a function of the vortex radius R/η. It is clear that these fluctuations become smaller as compressibility becomes stronger. It supports our view that contributions of vortices to generations of pressure fluctuation are suppressed by compressibility.

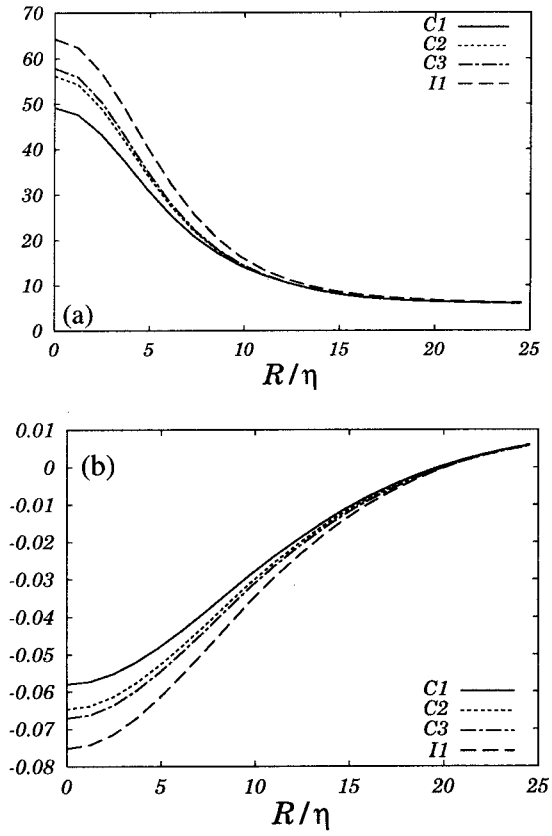

Figure 5: Averaged (a)longitudinal vorticity $\omega_{\|}$ and (b)incompressible part of the pressure p^I.

An mechanism of vortex suppression

An mechanism to suppress growth of vortex structures are investigated here. For this purpose, effects of density variations must be taken into account. Viscous effects is neglected for simplicity. The budget of the enstrophy density of an incompressible fluid is described by

$$\left(\frac{\partial}{\partial t} + \mathbf{u}\cdot\nabla\right)\frac{1}{2}|\omega|^2 = \omega\cdot\mathbf{S}\cdot\omega \tag{9}$$

where $\omega = \nabla\times\mathbf{u}$ is the vorticity. The compressible counterpart of eq.(9) is written in terms of the potential vorticity ω/ρ as

$$\left(\frac{\partial}{\partial t} + \mathbf{u}\cdot\nabla\right)\frac{1}{2}\left|\frac{\omega}{\rho}\right|^2 = \frac{\omega}{\rho}\cdot\mathbf{S}\cdot\frac{\omega}{\rho} + \frac{\nabla\rho\times\nabla p}{\rho^3}\cdot\frac{\omega}{\rho} \tag{10}$$

Since the baroclinic torques in our compressible runs are negligibly small, eqs.(9) and (10) coincide each other by replacing ω in eq.(9) by ω/ρ in eq.(10). It means that vortices of a compressible fluid are less stretched than those of an incompressible fluid even if the same strength of vortex stretching is imposed to them, because the stretching works

as much to change (decrease in this case) the density as to stretch vortices in a compressible fluid.

In Fig.6, time evolutions of squared potential vorticity $Q_\rho = \left\langle \left(\omega_\parallel/\rho\right)^2 \right\rangle_A /2$ are shown. (Recall that $\rho \equiv 1$ for an incompressible fluid.) The graphs collapse very well at the initial stage $t < 2$. We assert from this observation that some part of the vortex stretching are used to reduce density (namely, to make $1/\rho$ large) around vortex axes, not to stretch vortices.

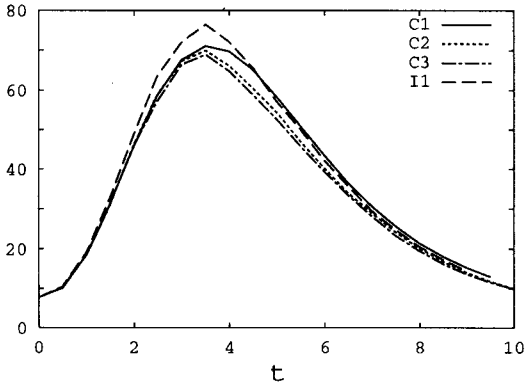

Figure 6: Time evolutions of the potential vorticity averaged on the vortex axes, $\left\langle \left(\omega_\parallel/\rho\right)^2 \right\rangle_A /2$.

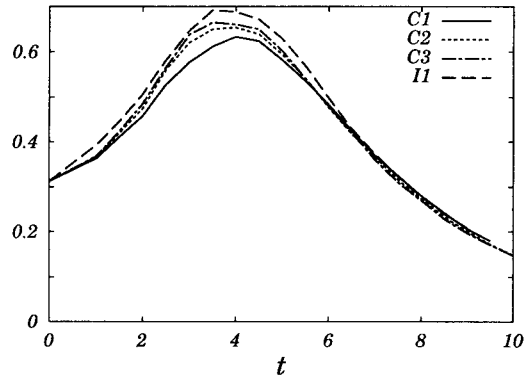

Figure 7: Time evolutions of the mean squared vortex stretching $\left\langle \left(\partial u_\parallel/\partial x_\parallel\right)^2 \right\rangle_A /2$

Though the suppression of longitudinal vorticity at the initial stage $t < 2$ is attributed to the density reduction, plots of Q_ρ do not collapse for $t > 2$. In the next stage $t > 2$, the suppression of swirling motions are not explained only by the density reduction effects and we have to find another mechanism to explain the vorticity reduction.

The growth of the longitudinal vorticity $\omega_\parallel$ is governed by the vortex stretching $\sigma = \partial u_\parallel/\partial x_\parallel$. In Fig.7 time evolutions of $\left\langle \sigma^2 \right\rangle_A$ are shown. The mean squared vortex stretching $\left\langle \sigma^2 \right\rangle_A$ decreases as compressibility becomes stronger. Though the amount of the reduction is not very large, the reduction of the vortex stretching works consecutively to suppress growth of $\omega_\parallel$.

One important candidate of the vortex stretching suppression is proposed here. Vortex structures are stretched and enhanced by the vortex stretching. Swirling motions of the enhanced vortices strengthen background shears and contribute to stretch other vortices. When the background shears are consumed to decrease density inside the vortices, vortices are not stretched very much. Then background shears are less strengthened and consequently, it fails to stretch vortices again. The process forms a sort of a cyclic mechanism and works to prohibit vortex structures growth.

In order for the cyclic mechanism to work effectively, vortices must be located sufficiently close to each other. In Fig.8(a), a vortex core and three vortex axes sticking into the core in run C1 are shown. In Fig.8(b), a vortex core of run I1 which shares the same ancestor in the initial condition with the core in Fig.8(a), is shown for later use. As is seen in Fig.8(a), the axes are located next to each other closely and it often happens that one vortex axis goes into other vortex cores. (Readers may also refer to Fig.6 of Kida and Miura(1998b), in which a vortex axis gouges the core of another axis.)

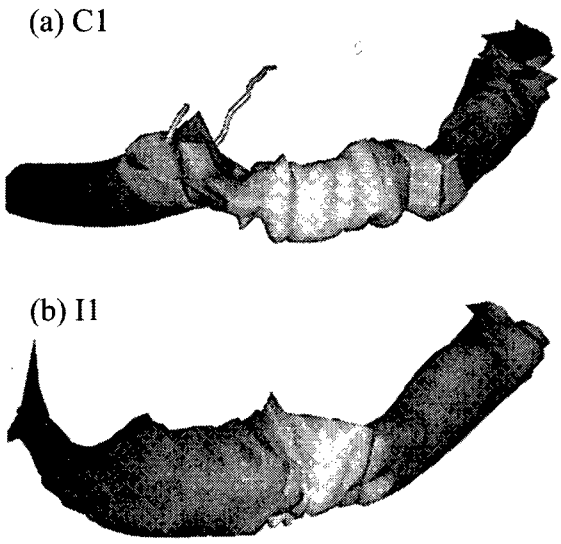

Figure 8: Typical close-views of (a)compressible and (b)incompressible vortex cores, which shares their ancestor in the initial condition.

By counting the length of vortex axes covered by other vortex cores, it is estimated that about from 5 to 20% (depending on the stage of the time evolution) of the total length of vortex axes are affected directly by the swirling motions of other vortices. Therefore, the cyclic reduction mechanism of the vortex stretching is considered to have significant importance on the vortex stretching reduction observed in Figs.7.

WAVES ON VORTICES

In this section, we observe detailed structures of individual vortex structures. In Figs.8, compressible and incompressible vortices are shown. We find that the vortex core in Fig.8(a) is thinner and wavy than the one in Fig.8(b). Such a kind of differences is widely observed among compressible and incompressible vortices which shares their ancestors.

In Fig.9(a), plots of the vortex stretching σ on vortex axes are shown. The four graphs in Fig.9(a) represent σ on vortex axes which share the same ancestor at the initial time. The abscissa represents the distance of the point from one end of the axes to the other end measured along the axes.

In Fig.9(b), a part of Fig.9(a) is magnified. We find that σ of compressible runs oscillate rapidly while that of run I1 varies very slowly. As compressibility becomes stronger, the mean level of σ on these axes becomes lower, being consistent with the observation in Figs.7. In other words, amplitudes of the rapid oscillations becomes smaller as compressibility becomes weaker and those of the slow, large-scale oscillations becomes larger.

Properties of the oscillations are quantitatively investigated by pdfs of the periods of the oscillations. The oscillation period Λ is defined as the distance of two peaks. Since these oscillations are observed as much on longitudinal vorticity as on vortex stretching, only plots of longitudinal vorticity are shown here. In Figs.10(a) and (b), linear and log-log plots of the pdfs are shown, respectively. On one hand, the pdf of the incompressible run I1 has a broad peak, the tail of which decays proportionally to $(\Lambda/\eta)^{-3/5}$. The existence of the power-law represents that there is no characteristic scale for Λ in I1. On the other hand, the pdfs of compressible runs have sharp peak around $\Lambda/\eta \simeq 12$, being essentially different from the pdf of run I1. Furthermore, the pdf of compressible runs do not look converging to I1 when compressibility becomes weaker. It suggests that the periods of the oscillations with $\Lambda/\eta \simeq 12$ are intrinsic to compressible fluids and it does not coincide with the properties of an incompressible fluid in the limit of zero Mach number.

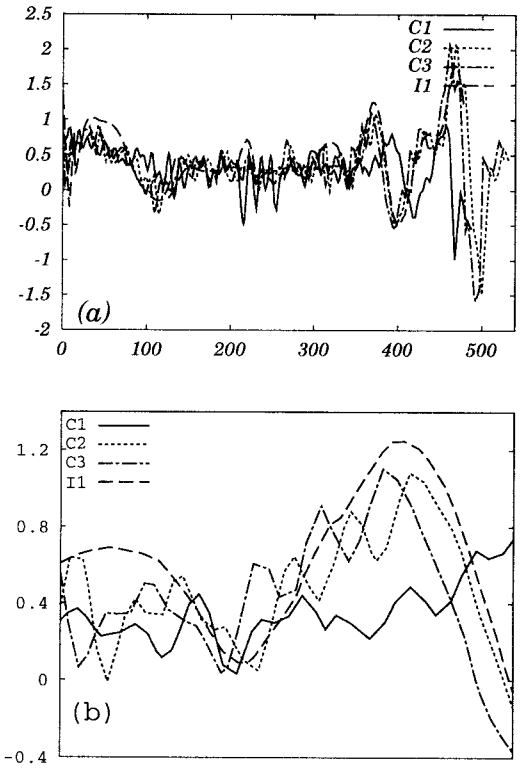

Figure 9: Oscillations observed on vortex axes.(a)Vortex stretching σ measured on the vortex axes which shares their ancestor in the initial condition. (b)A close-up view of (a).

CONCLUDING REMARKS

In this article, we have shown that strength of swirling motions of vortices are sensitive to compressible effects even though compressibility is not very strong. Density variations cause initial reduction of vortex enhancement and results to the reduction of vortex stretching by a sort of a cyclic mechanism. The existence of compressibility changes various properties of vortices. Especially, natures of waves observed on vortices are significantly changed by compressibility. Waves on incompressible vortices have been studied by Verzicco et al.(1995). In our DNS, large-scale oscillations which seem to have incompressible nature becomes weaker as compressibility becomes stronger, and small-scale oscillations become stronger in place of them.

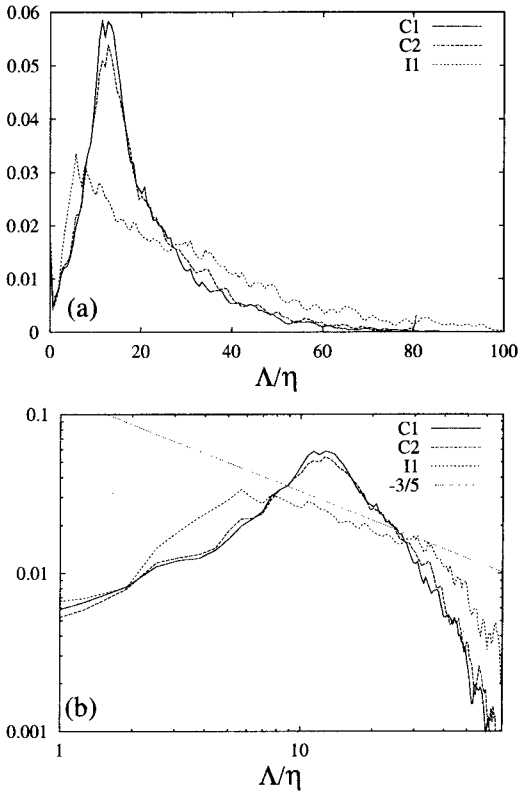

Figure 10: Pdfs of the periods of the oscillations in (a)linear and (b)log-log plots.

A detailed observations reveals that these oscillations are coupled with acoustic waves. (Figures for detailed time evolutions are omitted in this article.) Note that the waves on the vortex stretching consist both of compressible components (acoustic waves) and incompressible components. Our conjecture is that Kelvin waves (or inertial waves) are excited by the acoustic waves. Similar observations on acoustic/Kelvin waves have been reported by Kivotides et al.(2001) for superfluid turbulence. Our observations may be its counterpart only in normal fluid.

Finally, the observations on vorticity waves suggest that there are some properties which do not converge to an incompressible system in the zero-Mach number limit. It is worth conducting further investigation on compressible vortices to understand these nature of compressible turbulence.

The author thanks Professors S. Kida, T-H. Watanabe and Dr. S. Goto in NIFS for fruitful discussions. This work was partially supported by the Grant-in-Aid for Scientific Research for Encouragement of Young Scientists (B)(No.13750155) from Japan Society for the Promotion of Science, and the Grant-in-Aid for Scientific Research on Priority Area B(No.121225203) from the Ministry of Education, Culture, Sports, Science and Technology of Japan. Numer-

ical computations were carried out on the NEC SX-4 (till 2002) and SX-7 (since 2003) system in the Theory and Computer Simulation Center, NIFS.

REFERENCES

J. Jiménez, A. A. Wray, P. G. Saffman and R. S. Rogallo, 1993, "The structure of intense vorticity in isotropic turbulence", *J. Fluid Mech.* Vol. f255, pp. 65-90.

S. Kida and H. Miura, 1998a, "Swirl condition on a Low-Pressure Vortices", *J. Phys. Soc. Japan* Vol. 67, pp. 2166-2169.

S. Kida and H. Miura, 1998b, "Identification and Analysis of Vortical Structures", *Euro. J. Mech. B/Fluids* Vol. 17, pp. 471-488.

D. Kivotides, J. C. Vassilicons, D. C. Samuels and C. F. Barenghi, 2001, "Kelvin Waves Cascade in Superfluid Turbulence", *Phys. Rev. Lett.* Vol. 86, pp. 3080-3083.

S. Lee, S. K. Lele and P. Moin, 1991, "Eddy shocklets in decaying compressible turbulence", *Phys.Fluids A* Vol. 3 pp. 657-664.

S. K. Lele, "Compressibility effects on turbulence", *Ann. Rev. Fluid Mech.* Vol. 26, pp. 211-254.

H. Miura, 2002, "Analysis of vortex structures in compressible isotropic turbulence", *Comp. Phys. Comm.* Vol. 147, pp. 552-554.

H. Miura and S. Kida, 1997, "Identification of Tubular Vortices in Turbulence", *J. Phys. Soc. Japan* Vol. 66 pp. 1331-1334.

S. Sarkar, 1995, "The stabilizing effect of compressibility in turbulent shear flow", *J. Fluid Mech.* Vol. 282 pp. 163-186..

R. Verzicco, J. Jiménez and P. Orlandi, 1995, "On steady columnar vortices under local compression", *J. Fluid Mech.* Vol. 299, pp. 367-388.

A. W. Vreman et al, 1996, "Compressible mixing layer growth rate and turbulence characteristics", *J. Fluid Mech.* Vol. 320 235-258.